

On the homogeneity of SnIa absolute magnitude in the Pantheon+ sample

Leandros Perivolaropoulos^{1,*} and Foteini Skara^{1,†}

¹*Department of Physics, University of Ioannina, GR-45110, Ioannina, Greece*

(Dated: January 27, 2023)

We have analysed the Pantheon+ sample using a new likelihood model that replaces the single SnIa absolute magnitude parameter M used in the standard likelihood model of Brout et. al.[1] with two absolute magnitude parameters $M_<$, $M_>$ and a transition distance d_{crit} that determines the distance at which M changes from $M_<$ to $M_>$. The use of this likelihood dramatically changes the quality of fit to the Pantheon+ sample for a Λ CDM background by $\Delta\chi^2 = -19.6$ ($\Delta AIC = -15.5$ for two additional parameters). The tension between the $M_<$ and $M_>$ best fit values is at a level more than 3σ with a best fit d_{crit} very close to $20Mpc$. The origin of this improvement of fit and $M_< - M_>$ tension is that the new likelihood model, successfully models two signals hidden in the data: 1. The well known systematic effect called *volumetric redshift scatter bias* which is due to asymmetric peculiar velocity variations at redshifts $z < 0.01$ induced by unequal projected volumes at lower and higher distances compared to a given distance and 2. A mild signal for a change of intrinsic SnIa luminosity at about $20Mpc$. This interpretation of the results is confirmed by truncating the $z < 0.01$ Hubble diagram data from the Pantheon+ data where the above systematic is dominant and showing that the $M_< - M_>$ tension decreases from above 3σ to a little less than 2σ . It is also confirmed by performing a Monte Carlo simulation to compare the merged SnIa absolute luminosities M_i of SnIa+Cepheid hosts, obtained from the SH0ES data, with the anticipated luminosities in the context of a homogeneous single absolute magnitude M . This simulation shows that the maximum significance of the SnIa luminosity transition ($\Sigma \equiv \frac{|M_> - M_<|}{\sqrt{\sigma_{M_>}^2 + \sigma_{M_<}^2}}$) in the real data, is larger than the corresponding maximum significance of 94% of the corresponding homogeneous simulated samples.

I. INTRODUCTION

The value of the Hubble constant H_0 measured by direct local measurements based mainly on Type Ia supernovae (SnIa) standard candles calibrated using distance ladder methods is at 5σ tension with the corresponding value of H_0 measured indirectly using the sound horizon at last scattering as a standard ruler. This discrepancy constitutes one of the main challenges for the standard cosmological model Λ CDM known as the Hubble tension[2–4]

The most precise direct method for measuring the Hubble constant is based on observations of SnIa calibrated with Cepheid variable stars in galaxies that host both Cepheid variable stars and SnIa. Cepheids in turn are calibrated using geometric methods (e.g. parallax) in the Milky Way and other nearby anchor galaxies. This is the distance ladder method for the direct measurement of H_0 [5–9].

Such a distance ladder approach has been implemented recently by the SH0ES team (Supernovae and H0 for the Equation of State of dark energy) and has lead[8] to a best fit value $H_0^{R21} = 73.04 \pm 1.04 \text{ km s}^{-1} \text{ Mpc}^{-1}$ [8]. The corresponding indirect measurement of H_0 using the sound horizon at recombination as a standard ruler measured by the CMB perturbations angular power spectrum under the assumption of the validity of the standard cosmological model Λ CDM (inverse distance lad-

der approach) has lead to an even more precise value of $H_0^{P18} = 67.36 \pm 0.54 \text{ km s}^{-1} \text{ Mpc}^{-1}$ [10] (see also Refs. [2, 3, 11–19] for relevant recent reviews). The 5σ discrepancy (tension) between these two very precise measurements of H_0 indicates that most probably at least one of them is not accurate, because the assumptions on which it is based are not valid.

The local direct measurement of SH0ES is consistent with a wide range of other less precise local measurements of H_0 using alternative SnIa calibrators [20–23], gravitational lensing [24–27], gravitational waves [28–32], gamma-ray bursts as standardizable candles [33–37], quasars as distant standard candles [38], type II supernovae [39, 40], γ -ray attenuation [41] etc. (for recent reviews see Refs. [2, 3]).

The SH0ES measurement relies on the following assumptions:

- The measurements of the properties (period, metallicity) and luminosities of Cepheid calibrators and SnIa are accurate and free of unaccounted systematic errors.
- The modeling and physical laws involved in the calibration of Cepheids and SnIa in the three rungs of the distance ladder are accurate and well understood.

A recent analysis by the authors [42] has indicated that a simple variation of the Cepheid/SnIa modeling in the SH0ES analysis introducing a single new degree of freedom can potentially modify the best fit value of H_0 in such a way that it may become consistent with the corresponding inverse distance ladder measurement.

* leandros@uoi.gr

† f.skara@uoi.gr

This new degree of freedom allows for a transition of the SnIa calibrated and corrected intrinsic luminosity (absolute magnitude M) at some distance or redshift from a value $M_{<}$ at low distances (redshifts) to a value $M_{>}$ at high distances. It would therefore be interesting to introduce this new degree of freedom in the new extended Pantheon+ sample [1, 43, 44] which includes many more SnIa than the local SH0ES Cepheid+SnIa sample, to investigate if this degree of freedom is excited by the data.

The Pantheon+ SnIa luminosity sample [1, 43, 44] provides distance moduli derived from 1701 light curves of 1550 SnIa in a redshift range $z \in [0.001, 2.26]$ compiled across 18 different surveys. This sample is significantly improved over the first Pantheon sample of 1048 SnIa [45], especially at low redshifts z .

During the past few months when the Pantheon+ sample has been publicly available, a wide range of studies have investigated various aspects of it. In particular, the following aspects of Pantheon+ have been investigated: its consistency with the cosmological principle [46, 47], the self-consistency level of its covariance [48], its consistency with standard electromagnetism and gravity [49], the constraints it can provide on modified gravity and generalized dark energy [1, 50–54], the constraints it can provide on early dark energy [55, 56], the constraints it can provide on the start of cosmic acceleration [57], the constraints on possible modification of physics at recombination (e.g. electron mass variation) [58], the identification of possible change of the best fit value of H_0 when different redshift bins are considered [59–62], the effects of binning on its data [63–65], its consistency with BAO+BBN data [66], the constraints it implies on generalization of the Hubble law [67], constraints on compact object dark matter [68] etc.

One novel feature of Pantheon+ is that it may be used to infer H_0 in addition to cosmological parameters. This is due to the fact that it includes the distance moduli of SnIa in Cepheid hosts as obtained directly from the distance ladder analysis of SH0ES [8]. It also includes the covariance of these SnIa with the SnIa in the Hubble flow. The estimate of H_0 was not possible in the first Pantheon sample [45] because of the degeneracy between H_0 and SnIa absolute magnitude M . The inclusion of both the apparent magnitude m_B and the distance modulus from Cepheids μ_{Ceph} for SnIa in Cepheid hosts allows the independent determination of the absolute magnitude $M = m_B - \mu_{Ceph}$ which breaks the degeneracy between M and H_0 thus allowing the independent determination of H_0 through the Pantheon+ sample.

Due to the new features and data included in the Pantheon+ sample the following questions may be addressed:

- Is the best fit value of the SnIa absolute magnitude M consistent among various subsamples of the Pantheon+ sample?
- What is the effect of the introduction of new degrees of freedom (e.g. allowing for a change of M) on the quality of fit and on the best fit values of H_0

and cosmological parameters (e.g. matter density Ω_{0m})?

The goal of the present analysis is to address these questions focusing on the possible inhomogeneities of the standardized/corrected intrinsic luminosity (absolute magnitude) of the SnIa of the Pantheon+ sample as well as possible systematic effects like the *volumetric redshift scatter bias* [1, 69] discussed in Section III. Investigations of possible inhomogeneities of other properties of the SnIa (e.g. color or stretch parameters [70]) are also interesting but are beyond the scope of the present study.

The structure of this paper is the following: In the next section II we describe the data of the Pantheon+ sample that are relevant for our analysis and describe the method used for the fit of the cosmological parameters, the Hubble parameter H_0 and the SnIa absolute magnitude M . We then implement this method and obtain the corresponding best fit parameter values for Ω_{0m} , H_0 and M in the context of a Λ CDM background thus confirming the results of the original analysis of Brout et. al. [1] and verifying our implementation of the method described there. In section III, we generalize the model and the fitting method by allowing for a transition of the absolute magnitude parameter M at some distance d_{crit} from a value $M_{<}$ at distances $d < d_{crit}$ to a value $M_{>}$ at distances $d > d_{crit}$. We find the best fit parameter values for Ω_{0m} , H_0 , $M_{<}$ and $M_{>}$ with their uncertainties and test the consistency between the best fit values of $M_{<}$ and $M_{>}$ and carefully interpret the result taking also into account the volumetric redshift scatter bias. In section IV we discuss the statistical properties of the intrinsic luminosities M_i of SnIa in Cepheid hosts as obtained from the SnIa apparent magnitudes m_{Bi} and the Cepheid distance moduli μ_i^{Ceph} . Using Monte Carlo simulations and the Kolmogorov-Smirnov (KS) test [71], we check in particular the consistency of the statistical properties of the luminosities among different subsamples of the Pantheon+ [1] and SH0ES [8] samples. Finally in Section V we review our main results and discuss their interpretation and implications. We also point out possible future extensions of our analysis.

II. THE STANDARD ANALYSIS OF THE PANTHEON+ SAMPLE FOR Λ CDM

The Pantheon+ sample is presented through a table (Pantheon+SH0ES.dat) with 1701 rows (plus a header) which includes the data relevant to 1701 SnIa light curves in 47 columns which are described at [this url](#). It also consists of a 1701×1701 covariance matrix $C_{stat+sys}$ which represents the covariance between SnIa due to systematic and statistical distance moduli uncertainties as described below. The relevant columns for our analysis are the following:

- **Column 3:** Hubble Diagram Redshift (with CMB and peculiar velocity corrections).

- **Columns 9-10:** m_B corrected/standardized SnIa apparent magnitude and its uncertainty as obtained from the diagonal of the covariance matrix which also includes peculiar velocity induced, red-shift uncertainties.
- **Columns 11-12:** $\mu = m_B - M_{SH0ES}$ corrected/standardized distance moduli where the absolute SnIa magnitude $M_{SH0ES} = -19.253$ has been determined from SH0ES Cepheid host distances [8]. Its uncertainty as obtained from the diagonal of the covariance matrix is included in column 12. Column 11 is superfluous as it is trivially obtained from column 9 by subtracting M_{SH0ES} .
- **Column 13:** μ_{Ceph} corrected/standardized distance moduli of the SnIa hosts as obtained from the SH0ES distance ladder analysis [8] in the context of the H_0 distance ladder measurement. The uncertainty of μ_{Ceph} is not included in this Table but it is incorporated in the covariance matrix. This column has entries only in the rows which correspond to SnIa in Cepheid hosts. The rest of the rows have an entry '-9' in this column.
- **Column 14:** Takes the value 1 if the SnIa of the row is in Cepheid host and 0 otherwise.

In this section we follow [1] and use the above described Pantheon+ data to constrain the Hubble parameter $H_0 = 100 h \text{ km s}^{-1} \text{ Mpc}^{-1}$, the SnIa absolute magnitude M and the matter density parameter Ω_{0m} by minimizing a χ^2 likelihood:

$$\chi^2 = \vec{Q}^T \cdot (C_{\text{stat+sys}})^{-1} \cdot \vec{Q}, \quad (2.1)$$

where \vec{Q} is a vector with dimension 1701 and components which are usually defined as

$$Q_i = m_{Bi} - M - \mu_{\text{model}}(z_i), \quad (2.2)$$

where $m_{Bi} - M = \mu_i$ is the distance modulus of the i^{th} SnIa and $\mu_{\text{model}}(z_i)$ is the corresponding distance modulus as predicted by the assumed background cosmological model parametrization which in the present analysis is assumed to be Λ CDM. Thus we have

$$\mu_{\text{model}}(z_i) = 5 \log(d_L(z_i)/\text{Mpc}) + 25, \quad (2.3)$$

where the luminosity distance $d_L(z)$ is

$$d_L(z) = (1+z)c \int_0^z \frac{dz'}{H(z')}, \quad (2.4)$$

where c is the speed of light and in a Λ CDM background

$$H(z) = H_0 \sqrt{\Omega_M(1+z)^3 + \Omega_\Lambda}. \quad (2.5)$$

The parameters M and H_0 appear in Eqs. (2.1), (2.2) only through the combination $\mathcal{M} \equiv M - 5 \log(H_0 \cdot \text{Mpc}/c)$

and therefore they are degenerate and can not be estimated separately. In order to break this degeneracy, M can be estimated separately using the distance ladder approach by calibrating SnIa using Cepheids as was done with the previous Pantheon sample[72].

In the Pantheon+ sample this degeneracy is broken within the analysis by modifying the likelihood model (2.2) to include the distance moduli of SnIa in Cepheid hosts which can constrain M independently. Thus the vector \vec{Q} in the likelihood definition (2.2) is modified as follows [1]

$$Q'_i = \begin{cases} m_{Bi} - M - \mu_i^{\text{Ceph}} & i \in \text{Cepheid hosts} \\ m_{Bi} - M - \mu_{\text{model}}(z_i) & \text{otherwise,} \end{cases} \quad (2.6)$$

where μ_i^{Ceph} is the distance modulus of the Cepheid host of the i^{th} SnIa which is measured independently in the context of the distance ladder with Cepheid calibrators [8]. The novel feature of Pantheon+ is that the components Q'_i that correspond to SnIa in Cepheid hosts are now fully incorporated in the sample and correlated with the rest of the SnIa through the provided covariance matrix. Thus, the degeneracy between M and H_0 is broken and the three parameters M , H_0 and Ω_{0m} can be fit in the context of a Λ CDM background by minimizing

$$\chi^2(M, H_0, \Omega_{0m}) = \vec{Q}'^T \cdot (C_{\text{stat+sys}})^{-1} \cdot \vec{Q}', \quad (2.7)$$

where $C_{\text{stat+sys}}$ denotes the covariance matrix provided with the Pantheon+ data including both statistical and systematic uncertainties. We have obtained the best fit parameter values for M , H_0 and Ω_{0m} and constructed the $1\sigma - 3\sigma$ likelihood contours by minimizing χ^2 of Eq. (2.7) using a simple Mathematica v12 code which is publicly available.

The uncertainties for each one of the three best fit parameters were obtained using the square roots of the diagonal elements of the parameter covariance matrix which is the inverse of the Fisher matrix defined as

$$F_{ij} = \frac{1}{2} \frac{\partial^2 \chi^2(p_1, p_2, p_3)}{\partial p_i \partial p_j}, \quad (2.8)$$

where $i, j = 1, 2, 3$ and the parameters p_1, p_2, p_3 correspond to M , h and Ω_{0m} . We thus find

$$M = -19.25 \pm 0.03, \quad (2.9)$$

$$h = 0.734 \pm 0.01, \quad (2.10)$$

$$\Omega_{0m} = 0.333 \pm 0.018, \quad (2.11)$$

which is in excellent agreement with the best fit values for h and Ω_{0m} reported in [1]. The corresponding parameter likelihood contours are the blue contours shown in Figs. 1, 2.

At the minimum we also find $\chi_{\text{min}}^2 = 1522.98$ which corresponds to a χ^2 per degree of freedom of about 0.9. This is less than 1 and may indicate a possible overestimation of the uncertainties in the covariance matrix as pointed out recently in Ref. [48].

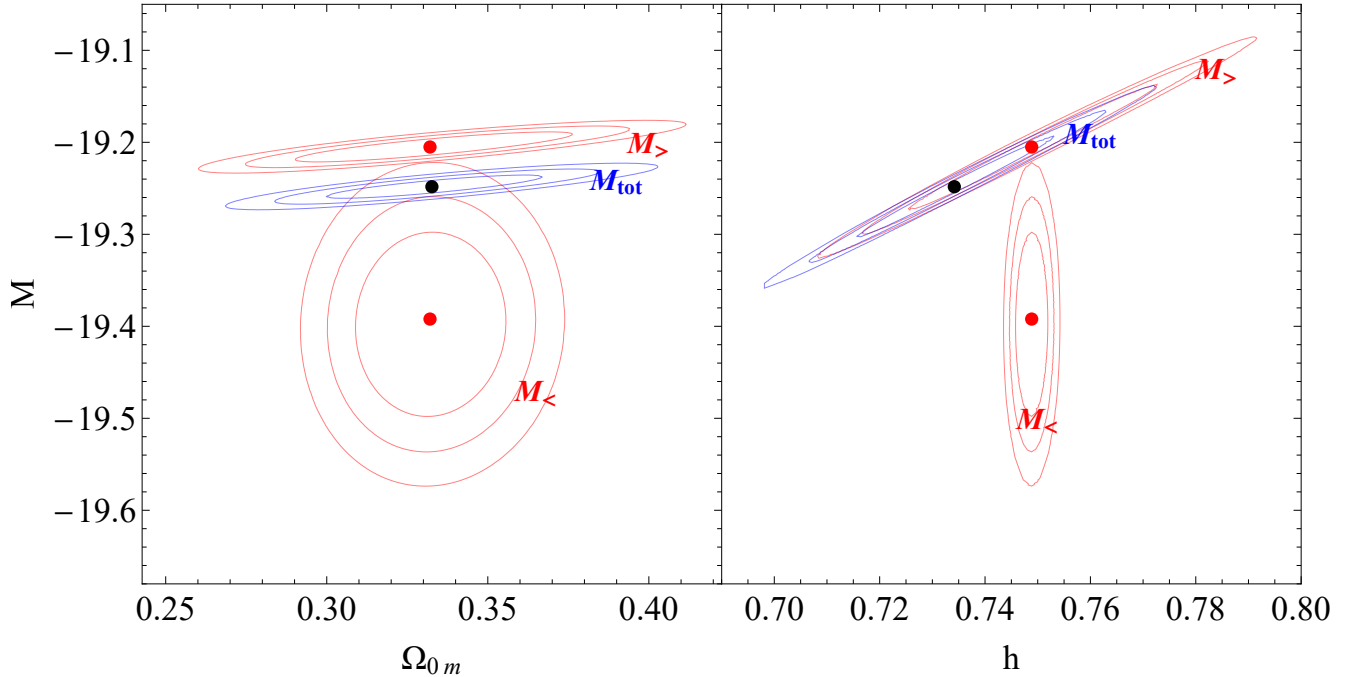


Figure 1. Blue contours: The $1-3\sigma$ likelihood contours for the parameters M , h and Ω_{0m} in the context of a Λ CDM background using the standard likelihood (2.6). Red contours: The $1-3\sigma$ likelihood contours for the parameters $M_{<}$, $M_{>}$, h and Ω_{0m} for a Λ CDM background in the context of the new likelihood model (3.2).

III. GENERALIZED ANALYSIS ALLOWING TRANSITION OF SNIa LUMINOSITY.

In order to test the homogeneity of the SNIa absolute magnitude parameter M , we now generalize the model of the previous section not by allowing more cosmological parameters but by allowing a change of the absolute magnitude at a distance d_{crit} such that it takes the form

$$M = \begin{cases} M_{<} & d < d_{crit} \\ M_{>} & d > d_{crit}, \end{cases} \quad (3.1)$$

The magnitude transition critical distance d_{crit} may be associated with a critical distance modulus through the relation $\mu_{crit} = 5 \log(d_{crit}/Mpc) + 25$. By introducing this degree of freedom in χ'^2 we obtain a generalized $\chi''^2(M_{<}, M_{>}, h, \Omega_{0m}, d_{crit})$ defined by using a vector \vec{Q}'' of the form

$$Q''_i = \begin{cases} m_{Bi} - M_{<} - \mu_i^{Cepheid} & \text{iff } \mu_{i,S} < \mu_{crit}, \text{ and } i \in \text{Cepheid hosts} \\ m_{Bi} - M_{>} - \mu_i^{Cepheid} & \text{iff } \mu_{i,S} > \mu_{crit}, \text{ and } i \in \text{Cepheid hosts} \\ m_{Bi} - M_{<} - \mu_{model}(z_i) & \text{iff } \mu_{i,S} < \mu_{crit}, \text{ and } i \notin \text{Cepheid hosts} \\ m_{Bi} - M_{>} - \mu_{model}(z_i) & \text{iff } \mu_{i,S} > \mu_{crit}, \text{ and } i \notin \text{Cepheid hosts}, \end{cases} \quad (3.2)$$

in the expression (2.1) for χ^2 . Here $\mu_{i,S} \equiv m_B - M_{SH0ES} \equiv m_B + 19.253$. Minimizing

$$\chi''^2(M_{<}, M_{>}, H_0, \Omega_{0m}, d_{crit}) = \vec{Q}''^T \cdot (C_{stat+sys})^{-1} \cdot \vec{Q}'' \quad (3.3)$$

with respect to the five indicated parameters we find the following best fit parameter values

$$M_{<} = -19.392 \pm 0.05, \quad (3.4)$$

$$M_{>} = -19.205 \pm 0.03, \quad (3.5)$$

$$h = 0.749 \pm 0.01, \quad (3.6)$$

$$\Omega_{0m} = 0.332 \pm 0.02, \quad (3.7)$$

$$d_{crit} = 19.95 \pm 0.1 Mpc, \quad (3.8)$$

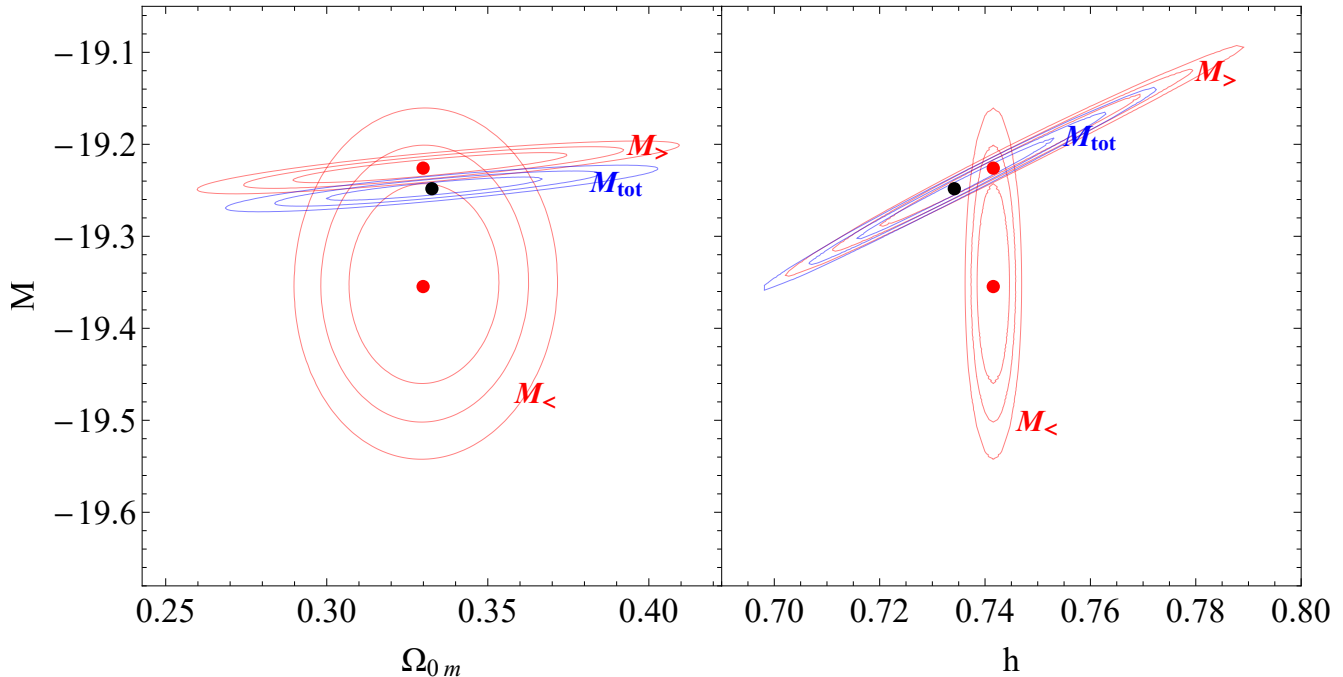


Figure 2. Same as Fig. 1 but using the likelihood model (3.9) which removes the Hubble diagram data with $z < 0.01$ to avoid the volumetric redshift scatter bias which tends to amplify possible intrinsic SnIa luminosity inhomogeneities in the data. As expected, the statistical significance of the apparent SnIa inhomogeneity has been significantly reduced but it has not disappeared.

with $\chi^2_{min} = 1503.38$. The corresponding likelihood contours are shown in Fig. 1. The quality of fit is significantly improved compared to the standard likelihood (2.7) with $\Delta\chi^2 = -19.6$ compared to the baseline model of [1] which has $\chi^2 = 1522.98$. Thus we have a reduction of the Akaike Information Criterion (AIC) by $\Delta AIC = -15.5$ for the model with 2 additional parameters d_{crit} and $M_{<}$ which is much larger than 6 and implies strong evidence for the transition model. Therefore the likelihood model (3.2) fits the Pantheon+ data much more efficiently than the standard likelihood (2.6) used by Brout et. al. [1]. As discussed below, there are two reasons for this improvement of the quality of fit: *the volumetric redshift scatter bias* and a mild evidence for an intrinsic transition of the SnIa absolute luminosity.

A well known systematic that may create an apparent inhomogeneity in the low redshift ($z < 0.01$) Hubble diagram data of the Pantheon+ sample is the *volumetric redshift scatter bias* [1, 69]. This is an asymmetric velocity variation of SnIa hosts between volumes at higher and lower distances compared to a given distance corresponding to a Hubble diagram redshift. A given velocity variation magnitude projects more galaxies to a given distance from a higher distance than from a lower distance because the higher distance volume is larger.

Thus, there are more galaxies at higher redshifts (where the volume is larger) projected to the correct Hubble diagram redshift due to a given peculiar velocity variation, compared to galaxies at lower redshifts where the volume is smaller. Due to this asymmetry, the Hubble diagram distance projected to a given redshift is higher than the real distance. This effect biases the measured distance modulus $\mu(z)$ to higher values (see eg the low z part of Fig. 4 of [1]) creating the impression of a lower SnIa absolute magnitude $M = m_B(z) - \mu(z)$ at $z < 0.01$ where the peculiar velocity noise compared to the Hubble flow is more important.

One way to deal with this bias is to fit for it with additional parameters in the likelihood model (eg $M_{<}$). In this case it may not be possible to distinguish this bias from a true physical variation of the SnIa intrinsic luminosity but it will significantly improve the quality of fit to the Pantheon+ data of all cosmological models.

An alternative approach would be to eliminate the effects of this bias (along with potentially useful information) by excluding Hubble diagram redshift datapoints at $z < 0.01$ from the fit of the low/high distance SnIa absolute magnitudes $M_{<}$, $M_{>}$. This may be achieved by the following likelihood model which removes all Hubble diagram data with $z < 0.01$:

$$Q_i''' = \begin{cases} m_{Bi} - M_{<} - \mu_i^{\text{Cepheid}} & \text{iff } \mu_{i,S} < \mu_{crit}, \text{ and } i \in \text{Cepheid hosts} \\ m_{Bi} - M_{>} - \mu_i^{\text{Cepheid}} & \text{iff } \mu_{i,S} > \mu_{crit}, \text{ and } i \in \text{Cepheid hosts} \\ 0 & \text{iff } z_i < 0.01 \\ m_{Bi} - M_{<} - \mu_{\text{model}}(z_i) & \text{iff } z_i > 0.01 \text{ and } \mu_{i,S} < \mu_{crit}, \text{ and } i \notin \text{Cepheid hosts} \\ m_{Bi} - M_{>} - \mu_{\text{model}}(z_i) & \text{iff } z_i > 0.01 \text{ and } \mu_{i,S} > \mu_{crit}, \text{ and } i \notin \text{Cepheid hosts,} \end{cases} \quad (3.9)$$

Thus, minimizing

$$\chi''''(M_{<}, M_{>}, H_0, \Omega_{0m}, d_{crit}) = \vec{Q}''''^T \cdot (C_{\text{stat}+\text{syst}})^{-1} \cdot \vec{Q}'''' \quad (3.10)$$

leads to the best fit parameter values

$$M_{<} = -19.355 \pm 0.05, \quad (3.11)$$

$$M_{>} = -19.226 \pm 0.03, \quad (3.12)$$

$$h = 0.74 \pm 0.01, \quad (3.13)$$

$$\Omega_{0m} = 0.33 \pm 0.02, \quad (3.14)$$

$$d_{crit} = 19.95 \pm 0.1 \text{ Mpc}, \quad (3.15)$$

The contours for this likelihood model are shown in Fig. 2 and we find $\chi_{min}^2 = 1445.7$ which is $\Delta\chi^2 = -7.5$ lower compared to the corresponding standard likelihood analysis (2.7) with the $z < 0.01$ datapoints removed. Thus we have a reduction of the Akaike Information Criterion (AIC) by $\Delta AIC = -3.5$ for the model (3.9) with 2 additional parameters d_{crit} and $M_{<}$ which is less than 6 but larger than 2 and implies mild evidence for the transition model even after the $z < 0.01$ datapoints are removed.

Based on the above new likelihood models, it becomes clear that at $d_{crit} \simeq 20 \text{ Mpc}$ there is a discrepancy between the best fit values parameter values $M_{<}$ and $M_{>}$ at a 3σ level. The discrepancy between these two parameters is partly due to the volumetric redshift scatter bias (which is not related to SNIa intrinsic luminosities) and partly due mild but persisting data hints for a transition of the SNIa intrinsic luminosities.

The modeling of this discrepancy with the introduced new degree of freedom induces no change in the best fit value of Ω_{0m} . However, some change is observed in the best fit value of h within its $1 - 2\sigma$ range (compare Eqs. (2.10) and (3.6)).

The question that raised therefore is the following: *Would other dynamical dark energy parameters be affected by the modeling of this discrepancy with new degrees of freedom?* The answer of this question is beyond the scope of the present analysis but if it is positive for some dynamical dark energy models, then the new likelihood model (3.2) which provides an overall much better quality of fit, may be preferable over the standard Pantheon+ likelihood model (2.6) for cosmological model fits.

The best fit value $M_{<}$ of the low distance SNIa absolute magnitude is fully consistent with the inverse distance ladder best fit value $M = -19.4 \pm 0.027$ [73] while the Hubble parameter best fit is about 1.5σ higher than the corresponding best fit value in the context of the standard likelihood (2.10). The best fit value of the transition

distance d_{crit} is consistent with corresponding results of previous studies [42, 74–76]¹ that have found hints for a transition of astrophysical properties including the parameters of the Tully-Fisher relation at a distance of about 20 Mpc .

In Ref. [42] it was pointed out that if the SH0ES data are reanalyzed by allowing for a change of the SNIa absolute magnitude at $d_{crit} = 50 \text{ Mpc}$ then the best fit value of the Hubble parameter shifts to a value almost identical with the inverse distance ladder best fit value albeit with significantly increased uncertainties. Motivated by this study we set $d_{crit} = 50 \text{ Mpc}$ ($\mu_{crit} = 33.5$) and minimize the generalized $\chi''''(M_{<}, M_{>}, h, \Omega_{0m})$. We thus find the following best fit parameter values with the corresponding 1σ uncertainties

$$M_{<} = -19.25 \pm 0.03, \quad (3.16)$$

$$M_{>} = -19.21 \pm 0.05, \quad (3.17)$$

$$h = 0.747 \pm 0.02, \quad (3.18)$$

$$\Omega_{0m} = 0.33 \pm 0.02, \quad (3.19)$$

with minor change of the quality of fit since $\chi_{min}'''' = 1522.28$ ($\Delta\chi_{min}'''' = -0.7$). Thus for $d_{crit} = 50 \text{ Mpc}$ we find no hint of discrepancy between $M_{<}$ and $M_{>}$ and thus no inhomogeneity with respect to the SNIa intrinsic luminosities. In addition no significant change is observed in the best fit value of h in contrast to the corresponding result for the SH0ES data analysis where the same degree of freedom induced a shift in the best fit value of h to $h = 0.67 \pm 0.04$. This may be due to the small number of SNIa in Cepheid hosts for the $M_{>}$ bin (4 SNIa) combined with the much larger number of SNIa in the Hubble flow bin for the Pantheon+ sample and the much more extensive covariance matrix.

IV. STATISTICAL PROPERTIES OF SNIa INTRINSIC LUMINOSITIES.

In this section we investigate the extend to which the discrepancy between the $M_{<}$ and $M_{>}$ parameters obtained in the previous section is due to a transition of the SNIa intrinsic luminosity or if it only due to the volumetric redshift scatter bias systematic. We thus focus on the particular subset of the Pantheon+ sample that corresponds to SNIa in Cepheid hosts and investigate the

¹ See e.g. Figs. 8, 9 of Ref. [42].

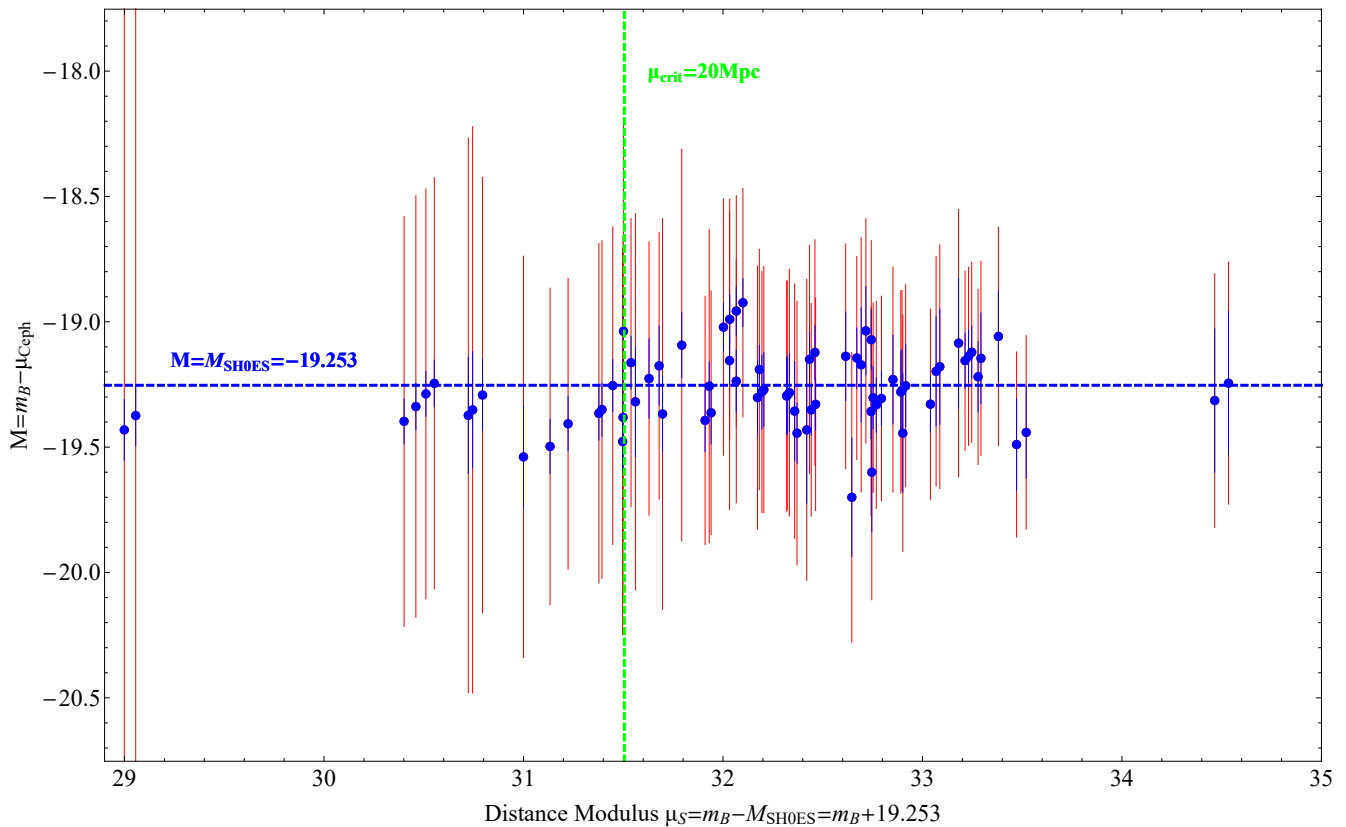


Figure 3. The absolute magnitudes of SnIa residing in Cepheid hosts as obtained from the Pantheon+ data. The best fit SnIa standardized and corrected absolute magnitudes and uncertainties based on the SH0ES analysis is also shown (blue dashed line). The inflated uncertainties of the Pantheon+ data are due to redshift uncertainties due to peculiar velocity noise. Notice that all datapoints below the distance $d_{crit} = 20 Mpc$ are below the best fit M_{SH0ES} line.

statistical properties of their individual absolute magnitudes. The measured absolute magnitude M_i of individual SnIa in Cepheid hosts can be directly obtained from the Pantheon+ data as

$$M_i = m_{B,i} - \mu_i^{\text{Ceph}} \quad (4.1)$$

i.e. by subtracting column 13 from column 9 for those entries where column 14 is 1. The inflated uncertainty of each M_i (red errorbar lines) is obtained from the corresponding entries of columns 10 and 13 only for plotting purposes as it will not be used in the statistical analysis of this section. This inflated uncertainty is not due to uncertainty of the SnIa luminosity but is due to the contribution of the peculiar velocity variation and its contribution to the redshift which should be taken into account in the Hubble diagram. It also is imposed to reduce the effect of the volumetric redshift scatter bias discussed in the previous section (for a more detailed discussion see Refs. [1, 69]).

In Fig. 3 we show a plot of the measured M_i for 77 SnIa light curves in Cepheid hosts vs the SnIa distance moduli $\mu_{S,i} = m_{B,i} - M_{SH0ES}$ (column 9) as obtained from the measured apparent magnitudes and the best fit value of M from SH0ES ($M_{SH0ES} = -19.253$, blue dashed line). We show both types of errorbars: The Pantheon+ error-

bars dominated by redshift uncertainties (red lines) and the SH0ES pure SnIa luminosity errorbars (blue lines) obtained using Table 6 of [8].

As shown in Fig. 3, SnIa at distances $d < 20 Mpc$ appear to be systematically more luminous (lower M_i) than the rest of the SnIa since almost all are below the blue dashed line corresponding to M_{SH0ES} ².

In order to compare the statistical properties of the M_i subsample with $d < 20 Mpc$ ($M_s^<$) with the corresponding distant subsample with $d > 20 Mpc$ ($M_s^>$) we show in Fig. 4 the probability distribution histogram of each subsample ($M_s^<$: dark blue columns, $M_s^>$: red columns, Full sample: green columns). As expected from Fig. 3 the probability distributions for the two subsamples differ significantly with $M_s^<$ being significantly skewed towards lower M values (brighter SnIa).

The statistical difference between the two subsamples may be quantified using a Kolmogorov-Smirnov test. Based on this test, the null hypothesis that the two sub-

² A similar trend appears for the four furthest SnIa with $d > 50 Mpc$ even though this is much less significant statistically. This is the origin of the effects observed in [42].

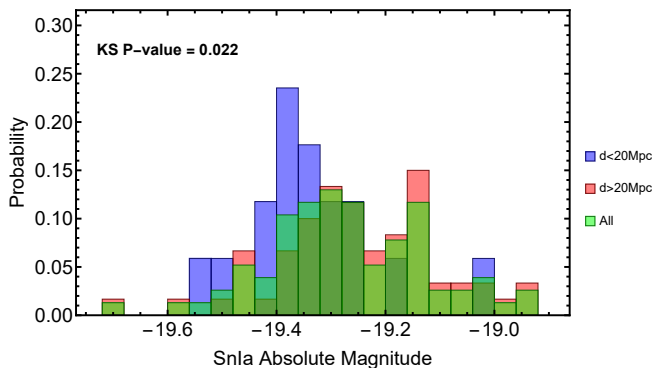


Figure 4. The probability distribution histogram of the absolute magnitudes of each SnIa subsample (Nearby subsample $M_s^<$: dark blue columns, Distant subsample $M_s^>$: red columns, Full sample of SnIa in Cepheid hosts: green columns)

samples have been drawn from the same probability distribution is rejected at the 2.5% level. In fact the probability that the two subsamples have been drawn from the same probability distribution is 2.2% (Kolmogorov-Smirnov P-value (KSPV))³ This result implies that a significant part of the $M_< - M_>$ discrepancy found in the previous section may be due to inhomogeneities in the SnIa corrected intrinsic luminosities of the Pantheon+ sample. This inhomogeneity could be due to either a large statistical fluctuation, or to an unaccounted systematic effect or to a physics transition that has occurred at a distance of about $20Mpc$ (about $70Myrs$ ago) [73, 77].

In the construction of the histogram of Fig. 4 we have implicitly assumed that the 77 absolute magnitudes of SnIa light curves shown in Fig. 3 are statistically independent. However, there are correlations among those light curves that refer to the same SnIa or to different SnIa in the same host.

In order to eliminate these correlations at the expense of ignoring some useful information, we consider the merged data corresponding to the same host using a weighted average, based on the uncertainties of each one of the 77 absolute magnitudes of Fig. 3. This weighted, host based, merging can also be obtained using the data in Table 6 of the SH0ES analysis [8].

We have thus reconstructed Fig. 5 using weighted binning (merging) of the absolute magnitudes in each host. The weighted binning in the j^{th} Cepheid+SnIa host of the SnIa/light curve absolute magnitudes was implemented by considering the absolute magnitude of the i^{th} SnIa/light curve in the j^{th} host galaxy ($j = 1 - 37$)

³ The distance scale used for this estimate is based on the Cepheid distance modulus μ_{Ceph} (Column 13 of the Pantheon+ data). If we use the distance scale μ_S shown in Fig. 3 (as done in all other parts of this analysis), the KSPV would be even smaller (KSPV = 0.001).

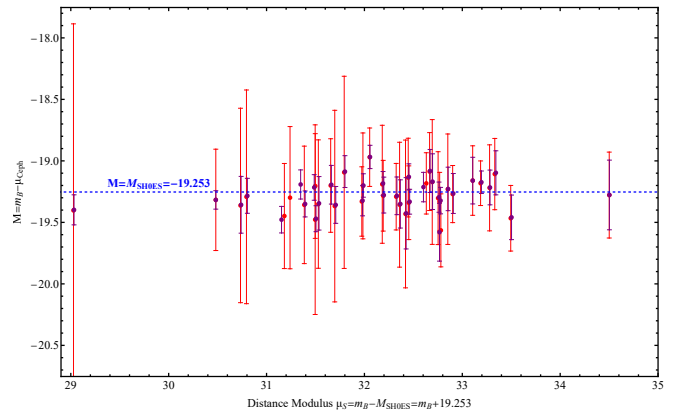


Figure 5. The merged absolute magnitudes of SnIa+Cepheid hosts as obtained from the Pantheon+ data (red points) and from the SH0ES data (Table 6 of [8], purple points). The agreement is good but the points are not fully identical. The increased errorbars of the Pantheon+ data are due to the peculiar velocity uncertainties needed for the cosmological fits.

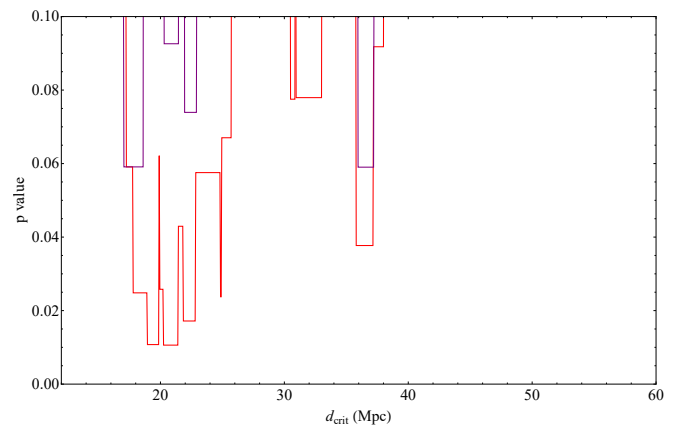


Figure 6. The KSPV comparing the two distance bins of the data shown in Fig. 5 as a function of d_{crit} that defines the two distance bins. The red line corresponds to the Pantheon+ merged data and the purple line corresponds to the SH0ES merged data.

and minimizing each $\chi^2(M_j)$ with respect to the M_j

$$\chi^2(M_j) = \sum_{i=1}^{N_j} \frac{(M_i - M_j)^2}{\sigma_{M_i}^2} \quad (4.2)$$

where N_j is the number of SnIa/light curves in the j^{th} Cepheid host galaxy. The 1σ range δM_j of each M_j was obtained by solving $\Delta\chi^2 = \chi^2(M) - \chi_{min}^2$ with $\Delta\chi^2 = 1$. This can be done analytically for the j^{th} host [78] leading to

$$M_j = \frac{\sum_{i=1}^{N_j} M_i / \sigma_i^2}{\sum_{i=1}^{N_j} 1 / \sigma_i^2} \quad (4.3)$$

$$\sigma^2(M_j) = \frac{1}{\sum_{i=1}^{N_j} 1 / \sigma_i^2} \quad (4.4)$$

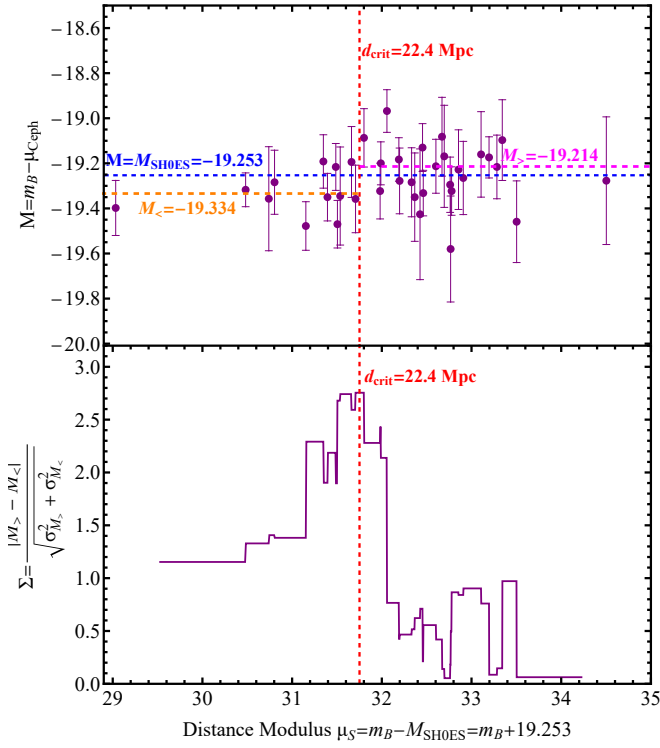


Figure 7. *Upper panel:* The 37 merged absolute magnitudes corresponding to the SnIa+Cepheid hosts obtained from Table 1 as a function of the SH0ES distance modulus μ_S . The distance $d_{crit} = 22.4 \text{ Mpc}$ corresponding to the maximum transition significance Σ_{max} is also indicated along with the corresponding values of $M_<$ and $M_>$ obtained from Eq. (4.5). *Lower panel:* The significance Σ of the $M_< - M_>$ transition as a function of the distance modulus $\mu_S^{crit} \equiv 5 \log_{10}(d_{crit}/\text{Mpc}) + 25$.

where the index i runs through the light curves or the SnIa of the j^{th} host. Using this merging method on the 77 light curve data shown in Fig. 3 or on the 42 SnIa shown in Table 6 of [8] we obtain the absolute magnitudes for each host shown in Fig. 5 obtained with the Pantheon+ data of Fig. 3 (red points) and from the SH0ES data (purple points, obtained using the data and uncertainties of Table 6 of [8]). The agreement between the two sources is very good with minor differences in a very small number of datapoints.

We now split the data in low and high distance bins split at a distance d_{crit} and compare the two bins to find the KSPV for each pair indicating the probability that the SnIa absolute magnitudes of each bin have been drawn from the same probability distribution. The resulting KSPV as a function of the splitting distance d_{crit} is shown in Fig. 6. The KSPV drops down to 0.01 for $d_{crit} \simeq 20 \text{ Mpc}$ for the Pantheon+ absolute magnitudes (red line) and down to 0.06 for the SH0ES absolute magnitudes of Fig. 5.

As an additional test of the homogeneity of the SnIa absolute magnitudes we investigate the statistical prop-

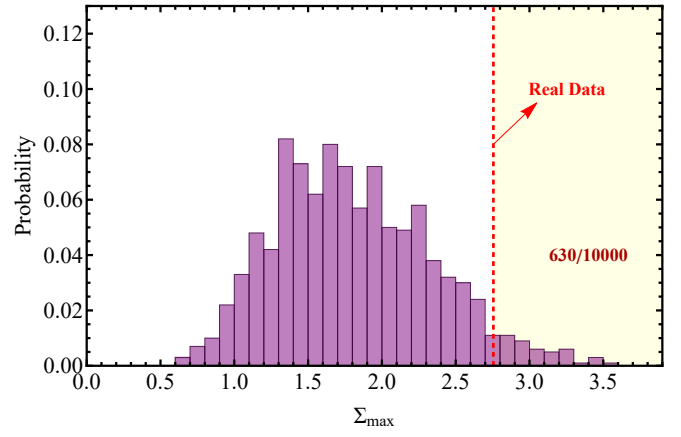


Figure 8. The probability histogram for the maximum transition significance Σ_{max} obtained from homogeneous simulated absolute magnitude data samples corresponding to the real data of Fig. 7 (upper panel). The Σ_{max} value of the real data is also shown.

erties of the significance Σ of the $M_< - M_>$ transition. The SH0ES merged host absolute magnitudes along with their uncertainties are plotted in the upper panel of Fig. 7 in terms of the merged SH0ES distance moduli defined as $\mu_{Si} \equiv m_{Bi} - M_{SH0ES} \equiv m_{Bi} + 19.253$ (upper panel). We then split these data in two distance bins according to a critical distance d_{crit} or a critical distance modulus $\mu_{crit} = 5 \log(d_{crit}/\text{Mpc}) + 25$. For the low distance bin $\mu < \mu_{crit}$ we obtain the weighted mean absolute magnitude $M_<$ and its uncertainty $\sigma^2(M_<)$ as

$$M_< = \frac{\sum_{i=1}^{N_k} M_i / \sigma_i^2}{\sum_{i=1}^{N_k} 1 / \sigma_i^2} \quad (4.5)$$

$$\sigma^2(M_<) = \frac{1}{\sum_{i=1}^{N_k} 1 / \sigma_i^2} \quad (4.6)$$

where the index i runs over the N_k low distance bin hosts. Similarly we also obtain the high distance bin absolute magnitude $M_>$ and its uncertainty $\sigma^2(M_>)$. Then for each value of μ_{crit} we find the transition significance defined as

$$\Sigma(\mu_{crit}) \equiv \frac{|M_> - M_<|}{\sqrt{\sigma_{M_>}^2 + \sigma_{M_<}^2}} \quad (4.7)$$

and plot $\Sigma(\mu_{crit})$ in the lower panel of Fig. 7 in terms of μ_S^{crit} . The maximum significance Σ_{max} is obtained for $d_{crit} = 22.4 \text{ Mpc}$ as $\Sigma_{max} = 2.75$ (lower panel of Fig. 7) with

$$M_<(d_{crit} = 22.4) = -19.33 \pm 0.04 \quad (4.8)$$

$$M_>(d_{crit} = 22.4) = -19.21 \pm 0.03 \quad (4.9)$$

These values are shown as dashed lines in the upper panel of Fig. 7 based on the 37 host merged SH0ES datapoints

shown in Table I which in turn is based on the 42 SnIa shown in Table 6 of [8].

Next we address the question: How often would this value of Σ_{max} or larger be obtained by chance in the context of Monte Carlo simulations generated under the assumption of homogeneous data with Gaussian variation around the best fit value of $M = M_{SHOES} = -19.253$ with the same uncertainties as the real data? Thus we generate 10000 such homogeneous simulated samples and vary d_{crit} in each of them (with step $\Delta d_{crit} = 0.2$) to determine the maximum transition significance $\Sigma_{max}(\mu_{crit})$ in each simulated sample. We find about that 630 such random samples (6.3% probability) have Σ_{max} larger or equal to the Σ_{max} of the real data. We conclude that the probability that a real transition signal is hidden in the SnIa absolute magnitudes of the data is about 94%. This probability would be somewhat lower if we had used the μ_{Ceph} (column 1 of Table I) distance scale instead of the μ_S (column 3 of Table I) distance scale in defining the $<$ and $>$ distance bins.

V. CONCLUSION-DISCUSSION

We have tested the internal consistency of the Pantheon+ sample with respect to the absolute magnitude parameter M . We have allowed for a change of M at some transition distance d_{crit} from $M_{<}$ at low distances (late times) to $M_{>}$ at high distances (early times). For $d_{crit} = 19.95 Mpc$, we found that such a change is favored by the Pantheon+ data leading to a reduction of χ^2 by $\Delta\chi^2_{min} = -19.6$ in the context of a Λ CDM cosmological background. This corresponds to reduction of the Akaike Information Criterion (AIC) by $\Delta AIC = -15.5$ (for two additional parameters). Such a reduction provides strong evidence that the model where a change of M is allowed, is very strongly preferred by the Pantheon+ data over the baseline model with a single value for M . This conclusion is further amplified by the fact that the best fit value of $M_{<}$ is in discrepancy with the best fit value of $M_{>}$ at a level of more than 3σ .

This effect is due at least partly, to the volumetric redshift scatter bias which is well known to exist in the data [1, 69] for Hubble diagram points with $z < 0.01$. We have tested the hypothesis that the $M_{<} - M_{>}$ discrepancy is due solely to this bias. We thus removed all Hubble diagram redshift datapoints with $z < 0.01$ from the Pantheon+ sample. We showed that the corresponding improvement of the fit reduces from $\Delta\chi^2 = -19.6$ to $\Delta\chi^2 = -7.5$. For the assumed two additional parameters this corresponds to $\Delta AIC = -3.5$ which indicates mild preference for an intrinsic SnIa absolute luminosity transition at $d_{crit} \simeq 20 Mpc$. The tension between the best fit parameters $M_{<}$ and $M_{>}$ also reduces to a little less than 2σ .

The probability of existence of an intrinsic transition of SnIa intrinsic luminosity in the Pantheon+ and SHOES data was also estimated using Monte Carlo simulations

to be about 94%. In addition, a Kolmogorov-Smirnov test has indicated that the probability that the absolute magnitudes M_i of SnIa in Cepheid hosts at distances $d < 22.4 Mpc$ are drawn from the same distribution as the M_i of SnIa at hosts with $d > 22.4 Mpc$ is less than 1.5%. This level of significance however, does not necessarily correspond to a transition of SnIa absolute luminosity and also is consistent with about 7% of homogeneous Monte Carlo data samples.

There are three main implications of our results:

New Likelihood Model: The likelihood (3.2) provides a much better fit to the Pantheon+ data than the standard likelihood (2.6) used in all current analyses of the Pantheon+ data. An important reason for this is the presence of the volumetric redshift scatter bias which is well fit by the new parameter $M_{<}$ in the (3.2) likelihood model. The use of this likelihood instead of the standard one of Brout et. al. [1] does not affect the best fit value of the cosmological parameter Ω_{0m} as shown by comparing Eqs. (2.11) and (3.7) but it does mildly affect the best fit value of the Hubble parameter h raising it from $h = 0.734 \pm 0.1$ to $h = 0.749 \pm 0.1$ (see Eqs. (2.10) and (3.6)). It may therefore affect other cosmological parameters of dynamical dark energy that are sensitive to low redshift cosmic dynamics. Hints for such an effect have been recently pointed out by [65] where it was shown that the deceleration parameter is affected by the presence of the $z < 0.01$ data of Pantheon+. For such cosmological models it may be more appropriate to use the likelihood (3.2) (or a generalized version of it) to fit the corresponding cosmological parameters. Thus a more detailed study of the effects of the new likelihood model on the best fit values of cosmological parameters would be an interesting extension of the present analysis.

Mild Evidence for Change of SnIa luminosity: The mild evidence for a transition of the SnIa absolute luminosity at a distance of about $20 Mpc$ requires further testing. If this possible SnIa luminosity inhomogeneity in the Pantheon+ and SHOES samples is due to a physics transition [77, 79–90] (e.g. gravitational transition [73, 91–95]), it may have implications for other calibration parameters like the color and stretch parameters. It would therefore be of interest to extend the present analysis in such directions by testing the homogeneity of the Pantheon+ sample with respect to possible differences of the best fit values of such parameters when these are allowed to change among different subsamples of the full Pantheon+ sample. Hints for such inhomogeneities from the first Pantheon sample have been already reported [70] with respect to the color and stretch parameters.

Implications for the Hubble tension: The best fit value $M_{<} = -19.33 \pm 0.04$ ⁴ of the low distance SnIa absolute magnitude is consistent with the inverse distance

⁴ In the absence of the volumetric redshift bias (no redshift points for $z < 0.01$).

ladder best fit value $M = -19.4 \pm 0.027$ [73]. This coincidence may have implications for the Hubble tension because if for some physical reason the best fit value of $M_{>}$ is not reliable and the true value of the SNIa luminosity is that implied by the best fit $M_{<}$ then the Hubble tension would be eliminated. In fact this observation may be related to the reduced tension found when calibrators at lower distances compared to Cepheids (like TRGB [96]) are used to calibrate SNIa. Thus the dependence the inferred SNIa absolute magnitude M_i , obtained from other SNIa calibrators like TRGB [96], on distance, should also be investigated to identify similar possible distance dependence on the calibration parameters.

As pointed out in previous studies, possible evolution of SNIa properties either in the form of a transition or in

the form of smooth evolution could significantly modify the values of cosmological parameters as obtained from data in different redshift bins [97–100]. Even if there is no real evolution of SNIa physical properties and the observed effect is purely due to volumetric redshift scatter bias or another systematic, its proper consideration in the likelihood through the likelihood model of Eq. (3.2) may play a role in the more accurate determination of cosmological parameters in the context of specific dynamical dark energy models with low z evolution. The investigation of this effect may be implemented by comparing the values of a wide range of cosmological dynamical dark energy models using the new likelihood (3.2) as an alternative to the standard Pantheon+ likelihood model (2.6).

NUMERICAL ANALYSIS FILES

The numerical files for the reproduction of the figures can be found [this Github repository under the MIT license](#).

ACKNOWLEDGMENTS

Special thanks are due to Adam Riess for extensive discussions and comments that significantly improved

our analysis and its interpretation. We also thank Eoin Colgain, Dan Scolnic and Dillon Brout for useful comments. This article is based upon work from COST Action CA21136 - Addressing observational tensions in cosmology with systematics and fundamental physics (CosmoVerse), supported by COST (European Cooperation in Science and Technology). This project was also supported by the Hellenic Foundation for Research and Innovation (H.F.R.I.), under the "First call for H.F.R.I. Research Projects to support Faculty members and Researchers and the procurement of high-cost research equipment Grant" (Project Number: 789).

-
- [1] Dillon Brout *et al.*, “The Pantheon+ Analysis: Cosmological Constraints,” *Astrophys. J.* **938**, 110 (2022), [arXiv:2202.04077 \[astro-ph.CO\]](#).
 - [2] Eleonora Di Valentino, Olga Mena, Supriya Pan, Luca Visinelli, Weiqiang Yang, Alessandro Melchiorri, David F. Mota, Adam G. Riess, and Joseph Silk, “In the realm of the Hubble tension—a review of solutions,” *Class. Quant. Grav.* **38**, 153001 (2021), [arXiv:2103.01183 \[astro-ph.CO\]](#).
 - [3] Leandros Perivolaropoulos and Foteini Skara, “Challenges for Λ CDM: An update,” *New Astron. Rev.* **95** (2022), [10.1016/j.newar.2022.101659](#), [arXiv:2105.05208 \[astro-ph.CO\]](#).
 - [4] L. Verde, T. Treu, and A. G. Riess, “Tensions between the Early and the Late Universe,” *Nature Astron.* **3**, 891 (2019), [arXiv:1907.10625 \[astro-ph.CO\]](#).
 - [5] Adam Riess, “SHOES-Supernovae, HO, for the Equation of State of Dark energy,” HST Proposal (2006).
 - [6] Adam G. Riess *et al.*, “A 2.4% Determination of the Local Value of the Hubble Constant,” *Astrophys. J.* **826**, 56 (2016), [arXiv:1604.01424 \[astro-ph.CO\]](#).
 - [7] Adam G. Riess, “The Expansion of the Universe is Faster than Expected,” *Nature Rev. Phys.* **2**, 10–12 (2019), [arXiv:2001.03624 \[astro-ph.CO\]](#).
 - [8] Adam G. Riess *et al.*, “A Comprehensive Measurement of the Local Value of the Hubble Constant with 1 km s⁻¹ Mpc⁻¹ Uncertainty from the Hubble Space Telescope and the SHOES Team,” *Astrophys. J. Lett.* **934**, L7 (2022), [arXiv:2112.04510 \[astro-ph.CO\]](#).
 - [9] Wendy L. Freedman, Barry F. Madore, Victoria Scowcroft, Chris Burns, Andy Monson, S. Eric Persson, Mark Seibert, and Jane Rigby, “Carnegie hubble program: A mid-infrared calibration of the hubble constant,” *Astroph. J.* **758**, 24 (2012).
 - [10] N. Aghanim *et al.* (Planck), “Planck 2018 results. VI. Cosmological parameters,” *Astron. Astrophys.* **641**, A6 (2020), [Erratum: *Astron. Astrophys.* 652, C4 (2021)], [arXiv:1807.06209 \[astro-ph.CO\]](#).
 - [11] Elcio Abdalla *et al.*, “Cosmology intertwined: A review of the particle physics, astrophysics, and cosmology associated with the cosmological tensions and anomalies,” *JHEAp* **34**, 49–211 (2022), [arXiv:2203.06142 \[astro-ph.CO\]](#).
 - [12] Paul Shah, Pablo Lemos, and Ofer Lahav, “A buyer’s guide to the Hubble constant,” *Astron. Astrophys. Rev.* **29**, 9 (2021), [arXiv:2109.01161 \[astro-ph.CO\]](#).
 - [13] Lloyd Knox and Marius Millea, “The Hubble Hunter’s Guide,” (2019), [arXiv:1908.03663 \[astro-ph.CO\]](#).

Table I. The SNIa+Cepheid host merged SH0ES data used for the construction of Figs. 5 and 7. The line corresponds to the $d_{crit} = 22.4Mpc$ as obtained from the μ_S column.

N	Host	μ_{Ceph} [mag]	σ [mag]	μ_S^a [mag]	σ [mag]	M [mag]	σ [mag]	m_B [mag]	σ [mag]
1	M101	29.178	0.041	29.033	0.119	-19.398	0.122	9.78	0.115
2	N5643	30.546	0.052	30.482	0.062	-19.317	0.075	11.229	0.054
3	N4424	30.844	0.128	30.740	0.194	-19.357	0.231	11.487	0.192
4	N4536	30.835	0.05	30.804	0.136	-19.284	0.142	11.551	0.133
5	N1365	31.378	0.056	31.153	0.097	-19.478	0.108	11.9	0.092
6	N1448	31.287	0.037	31.348	0.116	-19.192	0.118	12.095	0.112
7	N1559	31.491	0.061	31.394	0.091	-19.35	0.105	12.141	0.086
8	N2442	31.45	0.064	31.487	0.087	-19.216	0.104	12.234	0.082
9	N3982	31.722	0.071	31.505	0.084	-19.47	0.105	12.252	0.078
10	N7250	31.628	0.125	31.536	0.181	-19.345	0.218	12.283	0.178
11	N4038	31.603	0.116	31.662	0.11	-19.194	0.157	12.409	0.106
12	N4639	31.812	0.084	31.707	0.128	-19.358	0.15	12.454	0.124
13	N3972	31.635	0.089	31.801	0.099	-19.087	0.129	12.548	0.094
14	N2525	32.051	0.099	31.981	0.08	-19.323	0.124	12.728	0.074
15	N3447	31.936	0.034	31.989	0.094	-19.2	0.095	12.736	0.089
16	N5584	31.772	0.052	32.057	0.085	-18.968	0.095	12.804	0.079
17	N3370	32.12	0.051	32.19	0.087	-19.183	0.097	12.937	0.082
18	N5861	32.223	0.099	32.198	0.111	-19.278	0.146	12.945	0.107
19	N5917	32.363	0.12	32.332	0.1	-19.284	0.153	13.079	0.095
20	N3021	32.464	0.158	32.367	0.12	-19.35	0.196	13.114	0.116
21	N4680	32.599	0.205	32.426	0.207	-19.426	0.29	13.173	0.205
22	N3254	32.331	0.076	32.454	0.08	-19.13	0.106	13.201	0.074
23	N1309	32.541	0.059	32.462	0.087	-19.332	0.101	13.209	0.082
24	N1015	32.563	0.074	32.603	0.099	-19.213	0.12	13.35	0.094
25	N7541	32.5	0.119	32.671	0.131	-19.082	0.175	13.418	0.128
26	N2608	32.612	0.154	32.696	0.169	-19.169	0.226	13.443	0.166
27	N3583	32.804	0.08	32.762	0.098	-19.295	0.123	13.509	0.093
28	N5728	33.094	0.205	32.767	0.119	-19.580	0.235	13.514	0.115
29	U9391	32.848	0.067	32.778	0.089	-19.323	0.107	13.525	0.084
30	N0691	32.83	0.109	32.855	0.142	-19.228	0.177	13.602	0.139
31	M1337	32.92	0.123	32.908	0.11	-19.265	0.162	13.655	0.106
32	N3147	33.014	0.165	33.107	0.098	-19.16	0.19	13.854	0.093
33	N5468	33.116	0.074	33.195	0.061	-19.174	0.091	13.942	0.054
34	N7329	33.246	0.117	33.283	0.085	-19.216	0.141	14.030	0.079
35	N7678	33.187	0.153	33.343	0.098	-19.097	0.179	14.09	0.093
36	N0976	33.709	0.149	33.503	0.107	-19.459	0.181	14.25	0.103
37	N0105	34.527	0.25	34.503	0.136	-19.277	0.283	15.25	0.133

Note: (a) The ranking order of the host galaxies in the table was made with increasing distance modulus μ_S (where $\mu_S = m_B - M_{SH0ES} = m_B + 19.253$)

- [14] Sunny Vagnozzi, “New physics in light of the H_0 tension: an alternative view,” *Phys. Rev. D* **102**, 023518 (2020), [arXiv:1907.07569 \[astro-ph.CO\]](#).
- [15] Mustapha Ishak, “Testing General Relativity in Cosmology,” *Living Rev. Rel.* **22**, 1 (2019), [arXiv:1806.10122 \[astro-ph.CO\]](#).
- [16] Edvard Mörtzell and Suhail Dhawan, “Does the Hubble constant tension call for new physics?” *JCAP* **1809**, 025 (2018), [arXiv:1801.07260 \[astro-ph.CO\]](#).
- [17] Dragan Huterer and Daniel L Shafer, “Dark energy two decades after: Observables, probes, consistency tests,” *Rept. Prog. Phys.* **81**, 016901 (2018), [arXiv:1709.01091 \[astro-ph.CO\]](#).
- [18] Jose Luis Bernal, Licia Verde, and Adam G. Riess, “The trouble with H_0 ,” *JCAP* **1610**, 019 (2016), [arXiv:1607.05617 \[astro-ph.CO\]](#).
- [19] Maria Dainotti, Biagio De Simone, Giovanni Montani, Tiziano Schiavone, and Gaetano Lambiase, “The Hubble constant tension: current status and future perspectives through new cosmological probes,” (2023) [arXiv:2301.10572 \[astro-ph.CO\]](#).
- [20] Wendy L. Freedman, “Measurements of the Hubble Constant: Tensions in Perspective,” (2021), [arXiv:2106.15656 \[astro-ph.CO\]](#).
- [21] Adrià Gómez-Valent and Luca Amendola, “ H_0 from cosmic chronometers and Type Ia supernovae, with Gaussian Processes and the novel Weighted Polynomial Regression method,” *JCAP* **04**, 051 (2018), [arXiv:1802.01505 \[astro-ph.CO\]](#).
- [22] D.W. Pesce *et al.*, “The Megamaser Cosmology Project. XIII. Combined Hubble constant constraints,” *Astrophys. J. Lett.* **891**, L1 (2020), [arXiv:2001.09213 \[astro-ph.CO\]](#).
- [23] Wendy L. Freedman, Barry F. Madore, Taylor Hoyt, In Sung Jang, Rachael Beaton, Myung Gyoon Lee, Andrew Monson, Jill Neeley, and Jeffrey Rich, “Calibration of the Tip of the Red Giant Branch (TRGB),” (2020), [arXiv:2002.01550 \[astro-ph.GA\]](#).
- [24] Kenneth C. Wong *et al.*, “H0LiCOW – XIII. A 2.4 per cent measurement of H_0 from lensed quasars: 5.3σ tension between early- and late-Universe probes,” *Mon. Not. Roy. Astron. Soc.* **498**, 1420–1439 (2020), [arXiv:1907.04869 \[astro-ph.CO\]](#).
- [25] Geoff C. F. Chen *et al.*, “A SHARP view of H0LiCOW: H_0 from three time-delay gravitational lens systems with adaptive optics imaging,” *Mon. Not. Roy. Astron. Soc.* **490**, 1743–1773 (2019), [arXiv:1907.02533 \[astro-ph.CO\]](#).
- [26] S. Birrer *et al.*, “TDCOSMO - IV. Hierarchical time-delay cosmography – joint inference of the Hubble constant and galaxy density profiles,” *Astron. Astrophys.* **643**, A165 (2020), [arXiv:2007.02941 \[astro-ph.CO\]](#).
- [27] S. Birrer *et al.*, “H0LiCOW - IX. Cosmographic analysis of the doubly imaged quasar SDSS 1206+4332 and a new measurement of the Hubble constant,” *Mon. Not. Roy. Astron. Soc.* **484**, 4726 (2019), [arXiv:1809.01274 \[astro-ph.CO\]](#).
- [28] M. Fishbach *et al.* (LIGO Scientific, Virgo), “A Standard Siren Measurement of the Hubble Constant from GW170817 without the Electromagnetic Counterpart,” *Astrophys. J. Lett.* **871**, L13 (2019), [arXiv:1807.05667 \[astro-ph.CO\]](#).
- [29] Kenta Hotokezaka, Ehud Nakar, Ore Gottlieb, Samaya Nissanke, Kento Masuda, Gregg Hallinan, Kunal P. Mooley, and Adam. T. Deller, “A Hubble constant measurement from superluminal motion of the jet in GW170817,” *Nature Astron.* **3**, 940–944 (2019), [arXiv:1806.10596 \[astro-ph.CO\]](#).
- [30] B. P. Abbott *et al.* (LIGO Scientific, Virgo, 1M2H, Dark Energy Camera GW-E, DES, DLT40, Las Cumbres Observatory, VINROUGE, MASTER), “A gravitational-wave standard siren measurement of the Hubble constant,” *Nature* **551**, 85–88 (2017), [arXiv:1710.05835 \[astro-ph.CO\]](#).
- [31] A. Palmese *et al.* (DES), “A statistical standard siren measurement of the Hubble constant from the LIGO/Virgo gravitational wave compact object merger GW190814 and Dark Energy Survey galaxies,” *Astrophys. J. Lett.* **900**, L33 (2020), [arXiv:2006.14961 \[astro-ph.CO\]](#).
- [32] M. Soares-Santos *et al.* (DES, LIGO Scientific, Virgo), “First Measurement of the Hubble Constant from a Dark Standard Siren using the Dark Energy Survey Galaxies and the LIGO/Virgo Binary–Black-hole Merger GW170814,” *Astrophys. J. Lett.* **876**, L7 (2019), [arXiv:1901.01540 \[astro-ph.CO\]](#).
- [33] Shulei Cao, Maria Dainotti, and Bharat Ratra, “Standardizing Platinum Dainotti-correlated gamma-ray bursts, and using them with standardized Amati-correlated gamma-ray bursts to constrain cosmological model parameters,” *Mon. Not. Roy. Astron. Soc.* **512**, 439–454 (2022), [arXiv:2201.05245 \[astro-ph.CO\]](#).
- [34] Shulei Cao, Maria Dainotti, and Bharat Ratra, “Gamma-ray burst data strongly favor the three-parameter fundamental plane (Dainotti) correlation relation over the two-parameter one,” (2022), [10.1093/mnras/stac2170](#), [arXiv:2204.08710 \[astro-ph.CO\]](#).
- [35] Maria Giovanna Dainotti, Giuseppe Sarracino, and Salvatore Capozziello, “Gamma-Ray Bursts, Supernovae Ia and Baryon Acoustic Oscillations: a binned cosmological analysis,” (2022), [10.1093/pasj/psac057](#), [arXiv:2206.07479 \[astro-ph.CO\]](#).
- [36] Maria Giovanna Dainotti, Via Nielson, Giuseppe Sarracino, Enrico Rinaldi, Shigehiro Nagataki, Salvatore Capozziello, Oleg Y. Gnedin, and Giada Bargiacchi, “Optical and X-ray GRB Fundamental Planes as cosmological distance indicators,” *Mon. Not. Roy. Astron. Soc.* **514**, 1828–1856 (2022), [arXiv:2203.15538 \[astro-ph.CO\]](#).
- [37] Maria Giovanna Dainotti, Vincenzo Fabrizio Cardone, Ester Piedipalumbo, and Salvatore Capozziello, “Slope evolution of GRB correlations and cosmology,” *Mon. Not. Roy. Astron. Soc.* **436**, 82 (2013), [arXiv:1308.1918 \[astro-ph.HE\]](#).
- [38] Guido Risaliti and Elisabeta Lusso, “Cosmological constraints from the Hubble diagram of quasars at high redshifts,” *Nature Astron.* **3**, 272–277 (2019), [arXiv:1811.02590 \[astro-ph.CO\]](#).
- [39] T. de Jaeger, L. Galbany, A. G. Riess, B. E. Stahl, B. J. Shappee, A. V. Filippenko, and W. Zheng, “A 5% measurement of the Hubble constant from Type II supernovae,” (2022), [10.1093/mnras/stac1661](#), [arXiv:2203.08974 \[astro-ph.CO\]](#).
- [40] T. de Jaeger, B.E. Stahl, W. Zheng, A.V. Filippenko, A.G. Riess, and L. Galbany, “A measurement of the Hubble constant from Type II supernovae,” (2020), [10.1093/mnras/staa1801](#), [arXiv:2006.03412](#)

- [astro-ph.CO].
- [41] Alberto Domínguez, Radosław Wojtak, Justin Finke, Marco Ajello, Kari Helgason, Francisco Prada, Abhishek Desai, Vaidehi Paliya, Lea Marcotulli, and Dieter Hartmann, “A new measurement of the Hubble constant and matter content of the Universe using extragalactic background light γ -ray attenuation,” (2019), [10.3847/1538-4357/ab4a0e](#), [arXiv:1903.12097 \[astro-ph.CO\]](#).
- [42] Leandros Perivolaropoulos and Foteini Skara, “A Reanalysis of the Latest SH0ES Data for H_0 : Effects of New Degrees of Freedom on the Hubble Tension,” *Universe* **8**, 502 (2022), [arXiv:2208.11169 \[astro-ph.CO\]](#).
- [43] Dan Scolnic *et al.*, “The Pantheon+ Analysis: The Full Data Set and Light-curve Release,” *Astrophys. J.* **938**, 113 (2022), [arXiv:2112.03863 \[astro-ph.CO\]](#).
- [44] Dillon Brout *et al.*, “The Pantheon+ Analysis: SuperCal-fragilistic Cross Calibration, Retrained SALT2 Light-curve Model, and Calibration Systematic Uncertainty,” *Astrophys. J.* **938**, 111 (2022), [arXiv:2112.03864 \[astro-ph.CO\]](#).
- [45] D. M. Scolnic *et al.* (Pan-STARRS1), “The Complete Light-curve Sample of Spectroscopically Confirmed SNe Ia from Pan-STARRS1 and Cosmological Constraints from the Combined Pantheon Sample,” *Astrophys. J.* **859**, 101 (2018), [arXiv:1710.00845 \[astro-ph.CO\]](#).
- [46] Jessica A. Cowell, Suhail Dhawan, and Hayley J. Macpherson, “Potential signature of a quadrupolar Hubble expansion in Pantheon+ supernovae,” (2022), [arXiv:2212.13569 \[astro-ph.CO\]](#).
- [47] Francesco Sorrenti, Ruth Durrer, and Martin Kunz, “The Dipole of the Pantheon+SH0ES Data,” (2022), [arXiv:2212.10328 \[astro-ph.CO\]](#).
- [48] Ryan Keeley, Arman Shafieloo, and Benjamin L’Huillier, “An Analysis of Variance of the Pantheon+ Dataset: Systematics in the Covariance Matrix?” (2022), [arXiv:2212.07917 \[astro-ph.CO\]](#).
- [49] Giuseppe Sarracino, Alessandro D. A. M. Spallicci, and Salvatore Capozziello, “Investigating dark energy by electromagnetic frequency shifts II: the Pantheon+ sample,” *Eur. Phys. J. Plus* **137**, 1386 (2022), [arXiv:2211.11438 \[astro-ph.CO\]](#).
- [50] Vivian Poulin, José Luis Bernal, Ely Kovetz, and Marc Kamionkowski, “The Sigma-8 Tension is a Drag,” (2022), [arXiv:2209.06217 \[astro-ph.CO\]](#).
- [51] Deng Wang, “Pantheon+ constraints on dark energy and modified gravity: An evidence of dynamical dark energy,” *Phys. Rev. D* **106**, 063515 (2022), [arXiv:2207.07164 \[astro-ph.CO\]](#).
- [52] S. A. Narawade and B. Mishra, “Phantom cosmological model with observational constraints in $f(Q)$ gravity,” (2022), [arXiv:2211.09701 \[gr-qc\]](#).
- [53] Reginald Christian Bernardo, Daniela Grandón, Jackson Levi Said, and Víctor H. Cárdenas, “Dark energy by natural evolution: Constraining dark energy using Approximate Bayesian Computation,” (2022), [arXiv:2211.05482 \[astro-ph.CO\]](#).
- [54] Suresh Kumar, Rafael C. Nunes, Supriya Pan, and Priya Yadav, “New late-time constraints on $f(R)$ gravity,” (2023), [arXiv:2301.07897 \[astro-ph.CO\]](#).
- [55] Marc Kamionkowski and Adam G. Riess, “The Hubble Tension and Early Dark Energy,” (2022), [arXiv:2211.04492 \[astro-ph.CO\]](#).
- [56] Théo Simon, Pierre Zhang, Vivian Poulin, and Tristan L. Smith, “Updated constraints from the effective field theory analysis of BOSS power spectrum on Early Dark Energy,” (2022), [arXiv:2208.05930 \[astro-ph.CO\]](#).
- [57] David Dahiya and Deepak Jain, “Revisiting the epoch of cosmic acceleration,” (2022), [arXiv:2212.04751 \[astro-ph.CO\]](#).
- [58] Nanoom Lee, Yacine Ali-Haïmoud, Nils Schöneberg, and Vivian Poulin, “What it takes to solve the Hubble tension through modifications of cosmological recombination,” (2022), [arXiv:2212.04494 \[astro-ph.CO\]](#).
- [59] X. D. Jia, J. P. Hu, and F. Y. Wang, “The evidence for a decreasing trend of Hubble constant,” (2022), [arXiv:2212.00238 \[astro-ph.CO\]](#).
- [60] Wang-Wei Yu, Li Li, and Shao-Jiang Wang, “First detection of the Hubble variation correlation and its scale dependence,” (2022), [arXiv:2209.14732 \[astro-ph.CO\]](#).
- [61] Maria Giovanna Dainotti, Biagio De Simone, Tiziano Schiavone, Giovanni Montani, Enrico Rinaldi, Gaetano Lambiase, Malgorzata Bogdan, and Sahil Ugale, “On the Evolution of the Hubble Constant with the SNe Ia Pantheon Sample and Baryon Acoustic Oscillations: A Feasibility Study for GRB-Cosmology in 2030,” *Galaxies* **10**, 24 (2022), [arXiv:2201.09848 \[astro-ph.CO\]](#).
- [62] Maria Giovanna Dainotti, Biagio De Simone, Tiziano Schiavone, Giovanni Montani, Enrico Rinaldi, and Gaetano Lambiase, “On the Hubble constant tension in the SNe Ia Pantheon sample,” *Astrophys. J.* **912**, 150 (2021), [arXiv:2103.02117 \[astro-ph.CO\]](#).
- [63] Eoin Ó. Colgáin, M. M. Sheikh-Jabbari, and Rance Solomon, “High Redshift Λ CDM Cosmology: To Bin or not to Bin?” (2022), [arXiv:2211.02129 \[astro-ph.CO\]](#).
- [64] Deng Wang, “Pantheon+ tomography and Hubble tension,” (2022), [arXiv:2207.10927 \[astro-ph.CO\]](#).
- [65] Erick Pastén and Victor Cárdenas, “Testing Λ CDM cosmology in a binned universe: anomalies in the deceleration parameter,” (2023), [arXiv:2301.10740 \[astro-ph.CO\]](#).
- [66] Nils Schöneberg, Licia Verde, Héctor Gil-Marín, and Samuel Brieden, “BAO+BBN revisited — growing the Hubble tension with a 0.7 km/s/Mpc constraint,” *JCAP* **11**, 039 (2022), [arXiv:2209.14330 \[astro-ph.CO\]](#).
- [67] Deng Wang, “Testing the Hubble law with Pantheon+,” (2022), [arXiv:2208.07271 \[astro-ph.CO\]](#).
- [68] S. Dhawan and E. Mörtzell, “Type Ia supernova constraints on compact object dark matter,” (2023), [arXiv:2301.10204 \[astro-ph.CO\]](#).
- [69] W. D’Arcy Kenworthy, Adam G. Riess, Daniel Scolnic, Wenlong Yuan, José Luis Bernal, Dillon Brout, Stefano Cassertano, David O. Jones, Lucas Macri, and Erik R. Peterson, “Measurements of the Hubble Constant with a Two-rung Distance Ladder: Two Out of Three Ain’t Bad,” *Astrophys. J.* **935**, 83 (2022), [arXiv:2204.10866 \[astro-ph.CO\]](#).
- [70] Radosław Wojtak and Jens Hjorth, “Intrinsic tension in the supernova sector of the local Hubble constant measurement and its implications,” (2022), [10.1093/mnras/stac1878](#), [arXiv:2206.08160 \[astro-ph.CO\]](#).
- [71] F. J. Massey, “The Kolmogorov-Smirnov test for goodness of fit,” *Journal of the American Statistical Association* **46**, 68–78 (1951).
- [72] D. M. Scolnic *et al.*, “The Complete Light-curve Sample of Spectroscopically Confirmed SNe Ia from Pan-

- STARRS1 and Cosmological Constraints from the Combined Pantheon Sample,” *Astrophys. J.* **859**, 101 (2018), [arXiv:1710.00845 \[astro-ph.CO\]](#).
- [73] Valerio Marra and Leandros Perivolaropoulos, “A rapid transition of G_{eff} at $z_t \simeq 0.01$ as a possible solution of the Hubble and growth tensions,” *Phys. Rev. D* **104**, L021303 (2021), [arXiv:2102.06012 \[astro-ph.CO\]](#).
- [74] George Alestas, Ioannis Antoniou, and Leandros Perivolaropoulos, “Hints for a Gravitational Transition in Tully–Fisher Data,” *Universe* **7**, 366 (2021), [arXiv:2104.14481 \[astro-ph.CO\]](#).
- [75] Leandros Perivolaropoulos and Foteini Skara, “Hubble tension or a transition of the Cepheid SnIa calibrator parameters?” *Phys. Rev. D* **104**, 123511 (2021), [arXiv:2109.04406 \[astro-ph.CO\]](#).
- [76] Leandros Perivolaropoulos, “Is the Hubble Crisis Connected with the Extinction of Dinosaurs?” *Universe* **8**, 263 (2022), [arXiv:2201.08997 \[astro-ph.EP\]](#).
- [77] George Alestas, Lavrentios Kazantzidis, and Leandros Perivolaropoulos, “ $w - M$ phantom transition at $z_t < 0.1$ as a resolution of the Hubble tension,” *Phys. Rev. D* **103**, 083517 (2021), [arXiv:2012.13932 \[astro-ph.CO\]](#).
- [78] William H. Press, Saul A. Teukolsky, William T. Vetterling, and Brian P. Flannery, *Numerical Recipes 3rd Edition: The Art of Scientific Computing*, 3rd ed. (Cambridge University Press, 2007).
- [79] G. Alestas, L. Perivolaropoulos, and K. Tanidis, “Constraining a late time transition of G_{eff} using low- z galaxy survey data,” (2022), [arXiv:2201.05846 \[astro-ph.CO\]](#).
- [80] Michael J. Mortonson, Wayne Hu, and Dragan Huterer, “Hiding dark energy transitions at low redshift,” *Phys. Rev. D* **80**, 067301 (2009), [arXiv:0908.1408 \[astro-ph.CO\]](#).
- [81] George Alestas, David Camarena, Eleonora Di Valentino, Lavrentios Kazantzidis, Valerio Marra, Savvas Nesseris, and Leandros Perivolaropoulos, “Late-transition versus smooth $H(z)$ -deformation models for the resolution of the Hubble crisis,” *Phys. Rev. D* **105**, 063538 (2022), [arXiv:2110.04336 \[astro-ph.CO\]](#).
- [82] Giampaolo Benevento, Wayne Hu, and Marco Raveri, “Can Late Dark Energy Transitions Raise the Hubble constant?” *Phys. Rev. D* **101**, 103517 (2020), [arXiv:2002.11707 \[astro-ph.CO\]](#).
- [83] Eleonora Di Valentino, Eric V. Linder, and Alessandro Melchiorri, “Vacuum phase transition solves the H_0 tension,” *Phys. Rev. D* **97**, 043528 (2018), [arXiv:1710.02153 \[astro-ph.CO\]](#).
- [84] Abdolali Banihashemi, Nima Khosravi, and Amir H. Shirazi, “Phase transition in the dark sector as a proposal to lessen cosmological tensions,” *Phys. Rev. D* **101**, 123521 (2020), [arXiv:1808.02472 \[astro-ph.CO\]](#).
- [85] Eleonora Di Valentino, Ricardo Z. Ferreira, Luca Visinelli, and Ulf Danielsson, “Late time transitions in the quintessence field and the H_0 tension,” *Phys. Dark Univ.* **26**, 100385 (2019), [arXiv:1906.11255 \[astro-ph.CO\]](#).
- [86] Ryan E. Keeley, Shahab Joudaki, Manoj Kaplinghat, and David Kirkby, “Implications of a transition in the dark energy equation of state for the H_0 and σ_8 tensions,” *JCAP* **12**, 035 (2019), [arXiv:1905.10198 \[astro-ph.CO\]](#).
- [87] Chiara Caprini *et al.*, “Detecting gravitational waves from cosmological phase transitions with LISA: an update,” *JCAP* **03**, 024 (2020), [arXiv:1910.13125 \[astro-ph.CO\]](#).
- [88] Marzieh Farhang and Nima Khosravi, “Phenomenological Gravitational Phase Transition: Reconciliation between the Late and Early Universe,” *Phys. Rev. D* **103**, 083523 (2021), [arXiv:2011.08050 \[astro-ph.CO\]](#).
- [89] K. Sato, “First Order Phase Transition of a Vacuum and Expansion of the Universe,” *Mon. Not. Roy. Astron. Soc.* **195**, 467–479 (1981).
- [90] Amol V. Patwardhan and George M. Fuller, “Late-time vacuum phase transitions: Connecting sub-eV scale physics with cosmological structure formation,” *Phys. Rev. D* **90**, 063009 (2014), [arXiv:1401.1923 \[astro-ph.CO\]](#).
- [91] Robert R. Caldwell, William Komp, Leonard Parker, and Daniel A. T. Vanzella, “A Sudden gravitational transition,” *Phys. Rev. D* **73**, 023513 (2006), [arXiv:astro-ph/0507622](#).
- [92] Nima Khosravi, Shant Baghran, Niayesh Afshordi, and Natacha Altamirano, “ H_0 tension as a hint for a transition in gravitational theory,” *Phys. Rev. D* **99**, 103526 (2019), [arXiv:1710.09366 \[astro-ph.CO\]](#).
- [93] Leandros Perivolaropoulos and Foteini Skara, “Gravitational transitions via the explicitly broken symmetron screening mechanism,” (2022), [arXiv:2203.10374 \[astro-ph.CO\]](#).
- [94] Leandros Perivolaropoulos, “ H_0 Crisis: Systematics of distance calibrators or The End of Λ CDM?” (), <https://www.youtube.com/watch?v=RQODU88A2ik&t=15s>.
- [95] Leandros Perivolaropoulos, “The tensions of the Λ CDM and a gravitational transition,” (), <https://www.youtube.com/watch?v=GKubKmPXDM8>.
- [96] Wendy L. Freedman *et al.*, “The Carnegie-Chicago Hubble Program. VIII. An Independent Determination of the Hubble Constant Based on the Tip of the Red Giant Branch,” (2019), [10.3847/1538-4357/ab2f73](#), [arXiv:1907.05922 \[astro-ph.CO\]](#).
- [97] Eoin Ó. Colgáin, M. M. Sheikh-Jabbari, Rance Solomon, Maria G. Dainotti, and Dejan Stojkovic, “Putting Flat Λ CDM In The (Redshift) Bin,” (2022), [arXiv:2206.11447 \[astro-ph.CO\]](#).
- [98] Eoin Ó. Colgáin, M. M. Sheikh-Jabbari, Rance Solomon, Giada Bargiacchi, Salvatore Capozziello, Maria Giovanna Dainotti, and Dejan Stojkovic, “Revealing intrinsic flat Λ CDM biases with standardizable candles,” *Phys. Rev. D* **106**, L041301 (2022), [arXiv:2203.10558 \[astro-ph.CO\]](#).
- [99] L. Kazantzidis, H. Koo, S. Nesseris, L. Perivolaropoulos, and A. Shafieloo, “Hints for possible low redshift oscillation around the best-fitting Λ CDM model in the expansion history of the Universe,” *Mon. Not. Roy. Astron. Soc.* **501**, 3421–3426 (2021), [arXiv:2010.03491 \[astro-ph.CO\]](#).
- [100] L. Kazantzidis and L. Perivolaropoulos, “Hints of a Local Matter Underdensity or Modified Gravity in the Low z Pantheon data,” *Phys. Rev. D* **102**, 023520 (2020), [arXiv:2004.02155 \[astro-ph.CO\]](#).